Redox Biology 52 (2022) 102292

Contents lists available at ScienceDirect

Redox Biology

journal homepage: www.elsevier.com/locate/redox

Glia maturation factor-β induces ferroptosis by impairing chaperone-mediated autophagic degradation of ACSL4 in early diabetic retinopathy

Caiying Liu [a,b], Wan Sun [a,b], Tong Zhu [a,b], Si Shi [a,b], Jieping Zhang [a,b], Juan Wang [a,b], Furong Gao [a,b], Qingjian Ou [a,b], Caixia Jin [a,b], Jiao Li [a,b], Jing-Ying Xu [a,b], Jingfa Zhang [c], Haibin Tian [a,b,***], Guo-Tong Xu [a,b,d,**], Lixia Lu [a,b,*]

[a] Department of Ophthalmology of Tongji Hospital and Laboratory of Clinical and Visual Sciences of Tongji Eye Institute, Tongji University School of Medicine, Shanghai, 200065, China
[b] Department of Biochemistry and Molecular Biology, School of Medicine, Tongji University, Shanghai, 200092, China
[c] Department of Ophthalmology, Shanghai General Hospital (Shanghai First People's Hospital), Shanghai Jiao Tong University, Shanghai, China
[d] The Collaborative Innovation Center for Brain Science, Tongji University, Shanghai, China

ARTICLE INFO

Keywords:
Glia maturation factor-β
Diabetic retinopathy
Ferroptosis
Chaperone-mediated autophagy

ABSTRACT

Diabetic retinopathy (DR) is one of the leading causes of blindness in the world, and timely prevention and treatment are very important. Previously, we found that a neurodegenerative factor, Glia maturation factor-β (GMFB), was upregulated in the vitreous at a very early stage of diabetes, which may play an important role in pathogenesis. Here, we found that in a high glucose environment, large amounts of GMFB protein can be secreted in the vitreous, which translocates the ATPase ATP6V1A from the lysosome, preventing its assembly and alkalinizing the lysosome in the retinal pigment epithelial (RPE) cells. ACSL4 protein can be recognized by HSC70, the receptor for chaperone-mediated autophagy, and finally digested in the lysosome. Abnormalities in the autophagy–lysosome degradation process lead to its accumulation, which catalyzes the production of lethal lipid species and finally induces ferroptosis in RPE cells. GMFB antibody, lysosome activator NKH477, CMA activator QX77, and ferroptosis inhibitor Liproxstatin-1 were all effective in preventing early diabetic retinopathy and maintaining normal visual function, which has powerful clinical application value. Our research broadens the understanding of the relationship between autophagy and ferroptosis and provides a new therapeutic target for the treatment of DR.

1. Introduction

Diabetic retinopathy (DR) is one of the leading causes of legal blindness in the world and results from blood–retina barrier (BRB) breakdown, neurodegeneration, glial dysfunction, and many other causes [1–3]. Retinal pigment epithelium (RPE) cells are located between the retinal neuroepithelial layer and the choroidal Bruch membrane, which can regulate the metabolism of retinal cell nutrients, secrete various growth factors to promote the growth of retina and choroidal cells, and engulf aging photoreceptor extracellular membrane discs through phagocytosis to ensure the normal function of photoreceptor cells [4,5]. Abnormalities in RPE cells are involved in the pathogenesis of DR via various pathways [3].

Autophagy is an important process resulting in lysosomal

Abbreviations: DR, diabetic retinopathy; GMFB, Glia maturation factor-β; CMA, chaperone-mediated autophagy; 4-HNE, 4-hydroxynonenal; LX-1, Liproxstatin-1; TEER, transepithelial electrical resistance; BafA1, Bafilomycin A1; RBCC, RPE-Bruch's membrane-choriocapillaris complex.

* Corresponding Author. Department of Ophthalmology of Tongji Hospital and Laboratory of Clinical and Visual Sciences of Tongji Eye Institute, Tongji University School of Medicine, Shanghai 200065, China
** Corresponding Author. Department of Ophthalmology of Tongji Hospital and Laboratory of Clinical and Visual Sciences of Tongji Eye Institute, Tongji University School of Medicine, Shanghai 200065, China
*** Corresponding Author. Department of Ophthalmology of Tongji Hospital and Laboratory of Clinical and Visual Sciences of Tongji Eye Institute, Tongji University School of Medicine, Shanghai 200065, China
E-mail address: lulixia@tongji.edu.cn (L. Lu).

https://doi.org/10.1016/j.redox.2022.102292
Received 6 February 2022; Received in revised form 8 March 2022; Accepted 15 March 2022
Available online 18 March 2022

degradation, which plays a vital role in retinal homeostasis [6,7]. The autophagic degradation of the shed photoreceptor outer segments is one of the most important functions of RPE cells. In addition, autophagy in RPE cells can delay the occurrence of diabetic retinopathy (DR) by regulating the mTOR pathway to regulate glycolipid metabolism and reduce oxidative stress, thereby reducing inflammation and clearing damaged mitochondria [8]. Retinal autophagy and the inflammatory response regulated by histone HIST1H1C/H1.2 have also been shown to be closely related to the development of DR [9].

Ferroptosis, a regulated cell death defined in 2012, has been found to be regulated by autophagy and is involved in various blinding diseases and pathophysiological states [10–12]. It occurs due to damage to the antioxidant capacity and an imbalance between the production and degradation of lipid active oxygen in cells, which eventually leads to membrane rupture and cell death. RPE ferroptosis induced by GSH depletion, exogenous oxidants, or direct ferrous iron supplementation was demonstrated to be a major pattern of oxidative stress-mediated RPE cell death [13–16]. Moreover, a recent study showed that NaIO3-induced ferroptosis is involved in the process of RPE cell degeneration during AMD modeling [17]. Although the accumulation of lipid peroxidation has also been found in the diabetic retina [18–21], the role of ferroptosis and its direct inducing mechanism are not yet known.

Since advanced DR can seriously damage vision and lead to irrecoverable blindness, timely prevention and treatment are very important. However, since the current treatments (e.g., laser photocoagulation, vitrectomy, anti-VEGF drugs, etc.) are mostly aimed at the late stage of the disease and have certain side effects and prognostic risks, research on the molecular mechanisms and treatments for the early pathogenesis is urgently needed. In our previous research, a neurodegenerative factor, Glia maturation factor-β (GMFB), was obviously upregulated in vitreous on the first day after the establishment of the diabetic rat model by STZ injection. Increasing evidence has supported that intracellular GMFB influences apoptosis and inflammation of several nerve cells [22–26], but there is little research on extracellular GMFB, which can be secreted under certain conditions [27,28]. The introduction of GMFB to the culture media can elicit some signaling and metabolic alterations in glioblastomas [29], which may act as a signaling molecule that influences signal transduction as well as cell communication via autocrine or paracrine fashions.

Here, we found that extracellular GMFB stimulated by high glucose can impact the lysosomal degradation process in autophagy through ATP6V1A translocation, which induces ACSL4 accumulation and ferroptosis in RPE cells and eventually disrupts the normal physiological function of the retina. We first revealed the role of chaperone-mediated autophagy (CMA) in degrading the ACSL4 protein and resisting ferroptosis. The application of GMFB antibody, lysosome activator NKH477, CMA activator QX77, or ferroptosis inhibitor Liproxstatin-1 (LX-1) in vivo were all effective in preventing early diabetic retinopathy and maintaining normal visual function.

Although the effects of autophagy on retina-related diseases have been reported, the direct or indirect effects are unclear and remain to be investigated. In addition, the role of GMFB in the retina has rarely been studied, and most studies focus on the effect of intracellular GMFB. Moreover, it has been found that ferroptosis is involved in oxidative stress-induced RPE cell death in vitro [30], but the direct inducing factor of ferroptosis in diabetic retinal cells remains unknown. Combined with the previous results, our findings will broaden the understanding of GMFB and the relationship between autophagy and ferroptosis, thus providing a new therapeutic target for the treatment of DR and other related diseases.

2. Results

1. High concentrations of GMFB in the vitreous damage the function of the retina and RPE cells

From our previous results, during a diabetic rat model construction, GMFB in the vitreous increased rapidly as early as one day after STZ injection (Fig. 1A). The high concentration of GMFB persisted for at least two weeks, which emphasizes its important role in early DR pathogenesis. It has been reported that GMFB is synthesized and localized mainly in Müller cells in the adult rat retina [31]. To verify whether Müller cells can secrete GMFB in response to high glucose stimulation, we treated a rat Müller cell line with 25 mM glucose and detected the GMFB content in the culture medium after ultrafiltration centrifugation. As envisaged, the GMFB concentration in the medium was significantly increased after 12 h of high glucose treatment (Fig. 1B).

To investigate the impact in vivo, 0.2 μg recombinant GMFB protein or an equal volume of PBS was injected into the vitreous of SD rats for 2/4 weeks. Injection of GMFB significantly disrupted the physiological function of the retina and induced neurodegeneration (Fig. 1C–E) but did not activate glial cells (Fig. 1F–G). Given that GMFB has been found to influence apoptosis and oxidative stress in several nerve cells, we also examined ROS levels in the retina after GMFB injection and found that the RPE cell layer was the primary site of action (Fig. 1H, Supplementary Fig. 1A).

To detect the impact in vitro, the expression pattern of ZO-1 and RPE65, as well as the transepithelial electrical resistance (TEER), were detected after GMFB treatment of ARPE19 cells. As previously hypothesized, cell interactions or junctions and RPE65 protein expression were effectively reduced after exposure (Fig. 1I–K, Supplementary Fig. 3A). Together, these results indicate that the high concentration of GMFB in the vitreous could damage the physiological function of the retina, especially RPE cells.

2. Extracellular GMFB induces ferroptosis in RPE cells

To identify genomic features and mechanisms associated with extracellular GMFB, we treated ARPE19 cells with GMFB for 4 h and performed RNA-seq expression-based GSEA analyses. Unexpectedly, many pathways related to ferroptosis were enriched in the differentially expressed genes after GMFB treatment (Fig. 2A, Supplementary Fig. 2). With transmission electron microscopy (TEM), we observed the distinctive morphological features of smaller mitochondria with increased membrane density in treated cells (Fig. 2B, mitochondria marked by red arrows), a phenomenon that has been reported to occur in ferroptotic cells [32]. To further investigate this finding, we examined the cell viability and protein expression levels of two acknowledged markers (ACSL4 and GPX4), all of which exhibited significant changes after GMFB treatment (Fig. 2C–D).

The core metabolic mechanisms of ferroptosis are lipid peroxidation and an imbalance of iron homeostasis. Extracellular GMFB increased lipid peroxidation, induced GSH deficiency and reduced active mitochondria (Fig. 2E–G) but did not influence the level of iron in ARPE19 cells (Supplementary Fig. 3B). In parallel, in vivo, the toxic lipid peroxidation product 4-hydroxynonenal (4-HNE) was also found to accumulate in the retina injected with GMFB (Fig. 2H, Supplementary Fig. 1B).

To further investigate whether GMFB impacts cell function through lipid peroxidation-induced ferroptosis, we pretreated ARPE19 cells with the inhibitor liproxstatin-1 (LX-1). LX-1 blocked GMFB-induced lipid peroxidation, GSH deficiency, and cell death (Figs. 2C and 4G) and showed significant protective effects on cell junctions (Fig. 2I–J, Supplementary Fig. 3C). Together, these results demonstrated that extracellular GMFB induces ferroptosis in RPE cells, which mainly manifests as lipid peroxidation and eventually impairs physiological function.

3. Extracellular GMFB induces lysosome dysfunction and autophagy blockage in RPE cells.

In addition to impaired mitochondria, unexpectedly, we also observed a large number of autophagic vacuoles with TEM in GMFB-

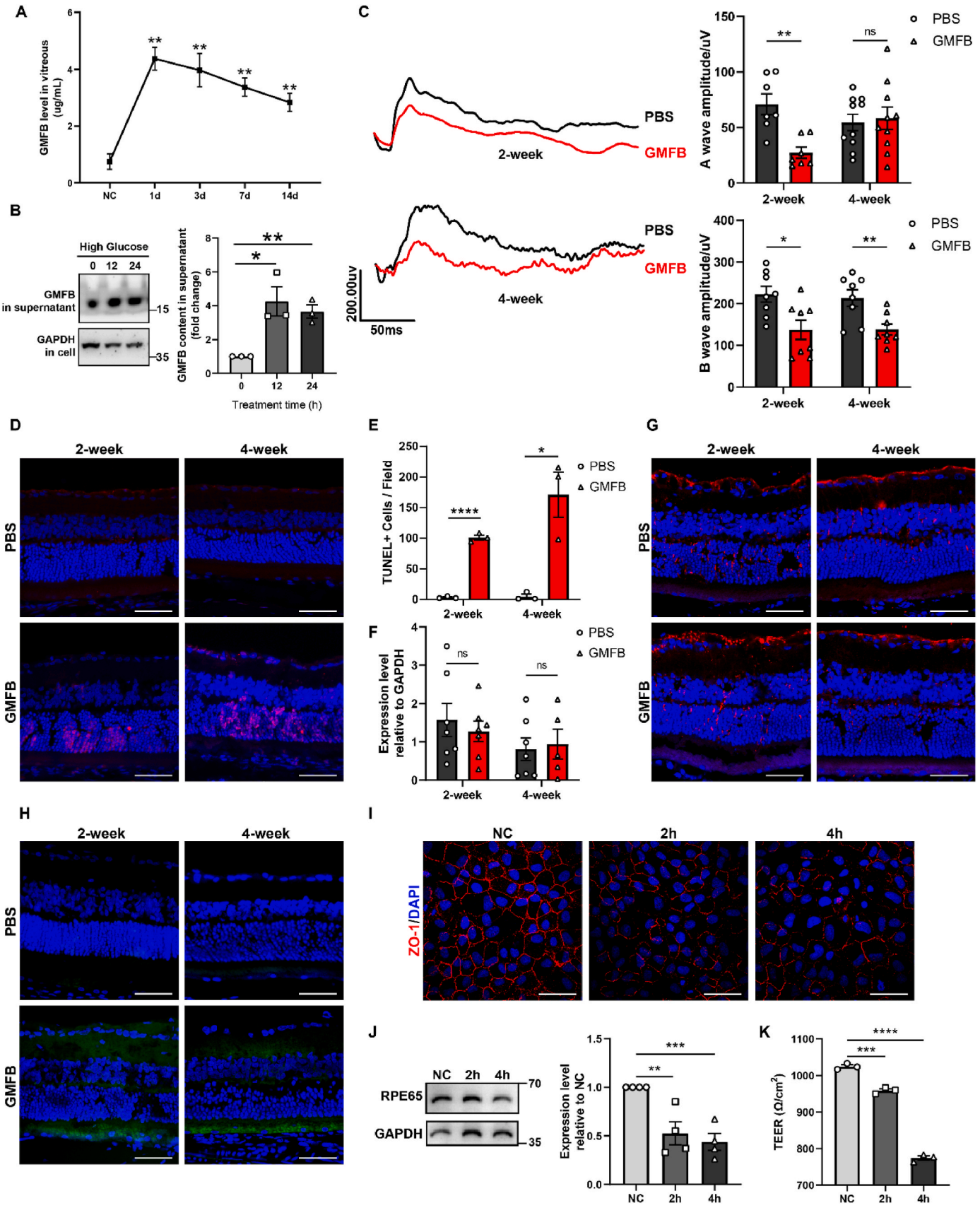

(caption on next page)

Fig. 1. High-concentration of GMFB in the vitreous damage the function of the retina and RPE cells
(A) The concentration of GMFB protein in the SD Rats' vitreous after injection with STZ for 1/3/7/14 days. (B) The content of GMFB protein in the supernatant of high glucose-treated rat Müller cells detected with Centrifugal Filter Devices and Western-blot. (C) The ERG result after injection of 0.2 μg GMFB or equal volume of PBS in SD Rats' vitreous for 2/4 weeks. (D–E) TUNEL-staining results of the SD Rats' retina after injection with GMFB for 2/4 weeks. (F–G) The expression of GFAP protein in the SD Rats' retina after GMFB injection detected with WB and IF staining. (H) The ROS level in the SD Rats' retina after GMFB injection detected with DCFH-DA ROS Assay Kit. (I) Immunofluorescence results of ZO-1 in ARPE19 cells after treatment with 0.01 μg/μL GMFB for different time. (J) The expression level of RPE65 in ARPE19 cells after treatment with 0.01 μg/μL GMFB for different time. (K) The transepithelial electrical resistance (TEER) of GMFB-treated RPE cells. Data are presented as means ± SEM of at least three independent experiments. *$p < 0.05$, **$p < 0.01$, ***$p < 0.001$ and ****$p < 0.0001$ versus the control with the same treatment (Student's t-test).

treated ARPE19 cells (Fig. 3A). The autophagic degradation of the shed photoreceptor outer segments is one of the most important functions of RPE cells. The increase in autophagosome number and P62 protein expression validated the impact of GMFB on autophagic flux (Fig. 3B–C). Consistent with the in vitro results, large amounts of autophagy-associated protein accumulated in the retina, especially the RPE layer, after GMFB injection (Fig. 3D–F).

Given that the degradation of P62 marks the normal function of autophagy, GMFB may impact the late stage of autophagy in ARPE19 cells, including autophagosome-lysosome fusion and lysosomal function. Immunofluorescence colocalization results did not show anomalies during autophagosome-lysosome fusion (Supplementary Fig. 4). However, as a result of Lysosome Tracker Red staining, GMFB treatment could damage the acidification and activity of lysosomes (Fig. 3G). The maintenance of a highly acidic pH is essential for the normal digestive function of lysosomes, which is generated mainly by the vacuolar H^+-ATPase (V-ATPase) complex [33]. Surprisingly, the ratio of the subunit ATP6V1A expression on the membrane was significantly decreased after GMFB treatment (Fig. 3H). Moreover, the ATPase activator NKH477 increased the acidity of lysosomes, thus inhibiting the accumulation of P62 (Figs. 3G and 4F). Together, these data suggest that extracellular GMFB impacts autophagic flux by injuring lysosomal function in RPE cells.

4. GMFB-induced lysosome dysfunction leads to ferroptosis through ACSL4 accumulation

To determine whether lysosome failure can induce ferroptosis in RPE cells, we treated cells directly with the ATPase inhibitor BafA1, which specifically inhibits lysosomal activity and induces the accumulation of P62 (Fig. 4A). As shown in Fig. 4B–E, BafA1 treatment significantly reduced cell viability and GSH concentration, increased ACSL4 expression and MDA levels in a time-dependent manner, and damaged mitochondria in RPE cells, all of which are features of ferroptosis. In contrast, the ATPase activator NKH477 increased the acidity and activity of lysosomes and protected autophagic flux, thus inhibiting the accumulation of P62 and ACSL4 (Fig. 4F). Similar to the hypothesis, NKH477 could also block GMFB-induced cell death, MDA production, and GSH deficiency, preventing the reduction in active mitochondria and cell tight junctions (Fig. 4G–K, Supplementary Fig. 3C). These results marked the importance of lysosome homeostasis in resisting ferroptosis and demonstrated that extracellular GMFB induces ferroptosis in RPE cells by obstructing autophagy–lysosome degradation.

Similar to extracellular GMFB, BafA1 treatment induced ferroptosis through lipid peroxidation but not through the imbalance of ferrous iron (Supplementary Fig. 3B). The protein ACSL4, which increases after GMFB or BafA1 treatment, can induce ferroptosis directly by catalyzing the generation of lethal lipid species [11]. Thus, we hypothesized that lysosomal dysfunction induces ferroptosis by upregulating ACSL4. Surprisingly, cells transfected with ACSL4-siRNA had significantly higher activity and lower MDA levels than the control group, even in the normal state, which were also resistant to GMFB- or BafA1-induced ferroptosis (Fig. 4L–O). Together, these results suggested that GMFB-induced lysosome failure led to ferroptosis in ARPE19 cells through upregulation of ACSL4.

5. ACSL4 is the substrate of chaperone-mediated autophagy (CMA)

The effect of GMFB on ACSL4 protein expression was not achieved through activation of transcription (Fig. 5A), which suggests that GMFB may up-regulate ACSL4 by impairing the degradation process in lysosomes. To verify this, we examined protein expression after CHX treatment with proteasome or lysosome inhibitors (Fig. 5B). It has been reported that in hepatic cells and primary cortical neurons, ACSL4 is degraded mainly through the proteasome pathway [34,35]. However, as previously hypothesized, the lysosome inhibitor CQ can also inhibit its degradation (Fig. 5B). The discrepancy with previous studies may be due to cell specificity or distinct disease context.

There are three forms of autophagy: macroautophagy, microautophagy, and CMA, all of which degrade substrates in lysosomes [36,37]. In ARPE19 cells, ACSL4 did not colocalize with P62, the receptor required for selective macroautophagy (Fig. 5C). However, there was obvious colocalization between ACSL4 and the CMA receptor LAMP2 or HSC70, which was also increased after GMFB treatment (Fig. 5D–E). To examine whether ACSL4 can be degraded by CMA, we treated ARPE19 cells with FBS-free culture medium or complete culture medium containing QX77, which can activate CMA by increasing the expression of LAMP2. Similar to the hypothesis, both of these methods promoted the degradation of ACSL4 (Fig. 5F). The recombinant plasmids ACSL4-Flag and HA-HSC70 were constructed to detect the combination directly through immunoprecipitation. The expression of HA-tag was found in the Flag-IP lysis of ARPE19 cells, and the addition of HSC70 also promoted the degradation of ACSL4 protein (Fig. 5G–H). The same results were also observed in HEK293T cells (Fig. 5I).

CMA only degrades soluble proteins bearing a KFERQ-like motif bound to HSC70 [37,38], and there are six possible KFERQ-like motifs in the ACSL4 protein sequence (shown in Fig. 5J). To functionally determine the most important motifs for recognition and degradation, we generated ACSL4 mutants with a 2-aa mutation in the hypothetical CMA motifs: ^{302}QCERI^{306} to ^{302}AAERI^{306}, ^{351}QSSKI^{355} to ^{351}AASKI^{355}, ^{407}KLEQI^{411} to ^{407}KLEAA^{411}, ^{566}QIIDR^{570} to ^{566}AAIDR^{570}, ^{574}LVKLQ^{578} to ^{574}LVKAA^{578}, and ^{629}QKGVE^{633} to ^{629}AAGVE^{633}. ACSL4 with mutated motifs ^{302}QCERI^{306}, ^{566}QIIDR^{570}, or ^{574}LVKLQ^{578} showed increased resistance to HSC70-induced degradation (Fig. 5K). Taken together, we conclude that ACSL4 is the substrate of chaperone-mediated autophagy, which can be recognized by the receptor HSC70 and degraded in the lysosome.

6. Retinal dysfunction induced by GMFB can be rescued with the CMA activator QX77 or the ferroptosis inhibitor LX-1

To confirm the role of CMA and ferroptosis in GMFB-induced retinopathy, we injected GMFB into the vitreous with the CMA activator QX77 and the ferroptosis inhibitor LX-1. Both drugs reduced neurodegeneration and presented a significant protective effect on the physiological function of the retina (Fig. 6A–B). The concentration of 4HNE and the expression of ACSL4 protein in the retina were also decreased after treatment (Fig. 6C–D). Unexpectedly, in the GMFB-injected group, there was also a significant increase in the level of GPX4, which is an antioxidant enzyme crucial in converting toxic lipid hydroperoxides to nontoxic alcohols [39]. This may be because GPX4 can also be degraded in the lysosome through CMA [40] or because compensatory effects

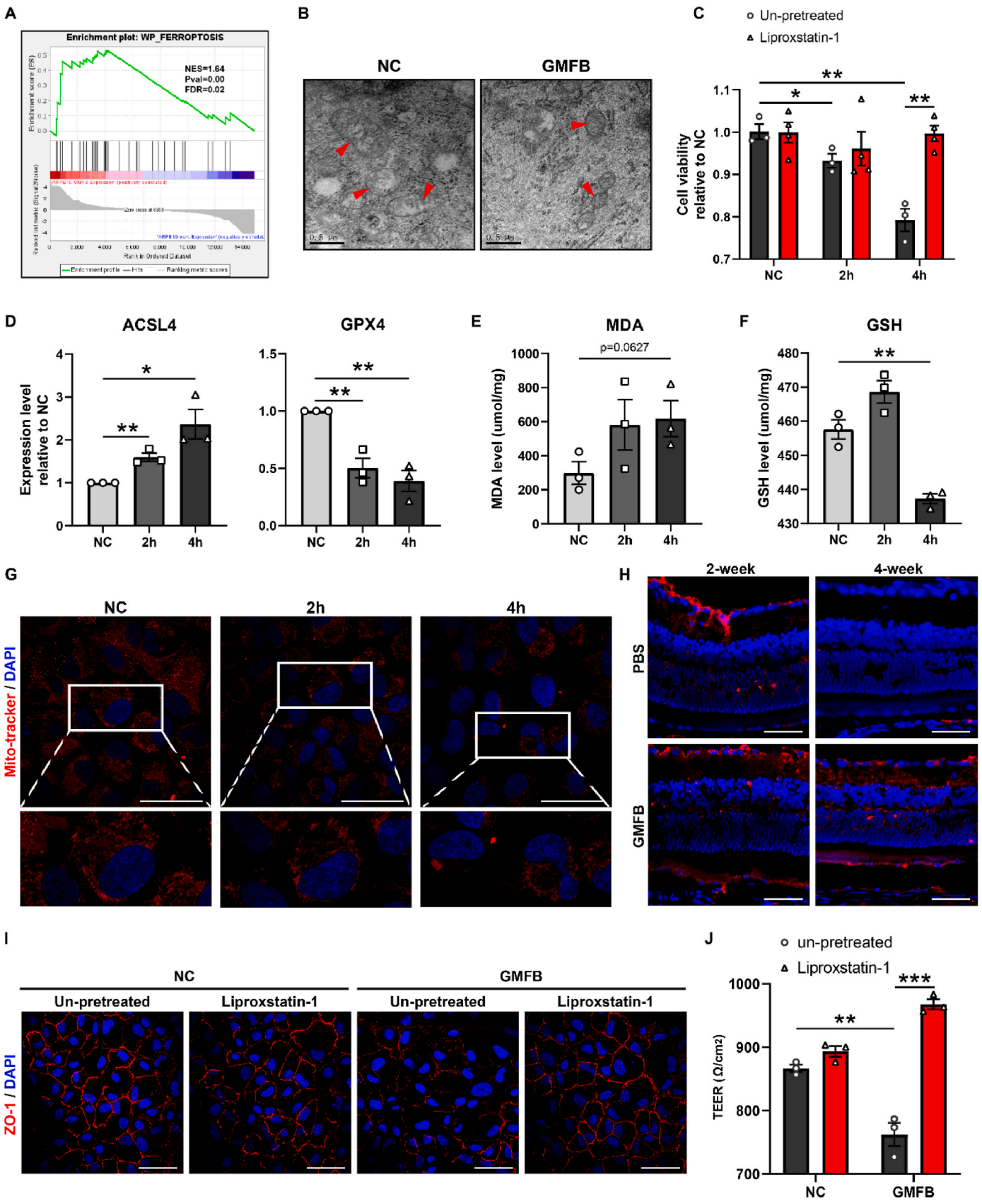

(caption on next page)

Fig. 2. Extracellular GMFB induces ferroptosis in RPE cells
(A) GSEA enrichment plot demonstrating the degree of correlation between genes in ferroptosis-associated gene sets and GMFB treatment. (B) Visualization of mitochondria in GMFB-treated ARPE19 cells by TEM. (C) The cell viability of ARPE19 cells after GMFB treatment with/without liproxstatin-1 detected with CCK-8. (D) The expression of ferroptosis relative protein in GMFB-treated ARPE19 cells detected through western-blot. (E–F) The MDA and GSH level in ARPE19 cells after treatment with 0.01 μg/μL GMFB for different time. (G) Active mitochondria stained with Chloromethyl-X-rosamine in GMFB-treated ARPE19 cells. Scale bar marks 20 μm. (H) Immunofluorescence results of 4-HNE in the SD Rats' retina after GMFB injection. Scale bar marks 50 μm. (I) Immunofluorescence results of ZO-1 in ARPE19 cells after GMFB treatment with/without liproxstatin-1. Scale bar marks 20 μm. (J) TEER of ARPE19 cells after GMFB treatment with/without liproxstatin-1. Data are presented as means ± SEM of at least three independent experiments. *p < 0.05, **p < 0.01, ***p < 0.001 versus the control with the same treatment (Student's t-test).

occur in complex retinal structures.

In general, we found that in a high glucose environment, large amounts of GMFB protein can be secreted in the vitreous, which translocates the ATPase ATP6V1A from the lysosome, preventing its assembly and alkalinizing the lysosome. The ACSL4 protein can be recognized by the CMA receptor HSC70 and finally digested in lysosomes. However, abnormalities in the degradation process lead to its accumulation, which can promote lipid peroxidation and ultimately induce ferroptosis in RPE cells (Fig. 6E).

7. GMFB antibody, QX77, NKH477, and LX-1 protects against DR

To validate the mechanism and explore new approaches for the treatment of early DR, we established a 2-week diabetic rat model and injected GMFB antibody (anti-GMFB), lysosome activator NKH477, CMA activator QX77, or ferroptosis inhibitor LX-1 into the vitreous on the first day of detectable hyperglycemia. Surprisingly, all drugs significantly rescued the physiological function of the retina, increasing the A- and B-waves almost to normal levels (Fig. 7A–B). Moreover, the expression of ACSL4 in the RPE-Bruch's membrane-choriocapillaris complex (RBCC), as well as the MDA level in the retina, both decreased in the drug-injected groups (Fig. 7C–D). For 4HNE, toxic lipid peroxidation, which has been reported to accumulate in the diabetic retina, was also reduced after drug injection (Fig. 7E).

In addition, we also measured autophagic flux in the RPE layer through immunofluorescence staining of P62 and LC3. All drugs, including LX-1, significantly reduced the number of autophagosomes, suggesting that Liproxstatin-1 may inhibit ferroptosis through a similar pathway (Fig. 7F). Together, GMFB antibody, NKH477, QX77, and LX-1 are all effective for preventing diabetic retinopathy in the early stage and protecting the normal function of the retina.

3. Discussion

The vitreous is a transparent gel that fills the posterior cavity of the eye and contains alternative proteins and polysaccharides, which play a vital role in the pathological events occurring in retinal tissue. In our previous research, a neurodegenerative factor, GMFB, was upregulated in the vitreous at a very early stage of diabetes, which may be secreted by retinal Müller cells and play an important role in the pathogenesis of DR. Here, we found that extracellular GMFB can damage lysosomal acidification in RPE cells, which leads to ACSL4 accumulation and ferroptosis and ultimately impairs the function of the retina. We first revealed the role of chaperone-mediated autophagy (CMA) in degrading ACSL4 protein and resisting ferroptosis. In a diabetic animal model, the application of GMFB antibody, lysosome activator NKH477, CMA activator QX77, and ferroptosis inhibitor Liproxstatin-1 (LX-1) all showed strong protective effects on retinal function, which have powerful clinical application value.

To investigate the function of GMFB in vivo, we injected chemosynthetic GMFB into the SD rat vitreous and found an impairment of physiological function (Fig. 1). Combined with the ROS results, we inferred that the fundus, especially RPE cells, is the primary site of action. In vitro, the results showing decreased cell junctions and RPE65 expression also validated this hypothesis. To identify the molecular mechanism, we performed RNA-seq expression-based GSEA analyses, and surprisingly found many ferroptosis-related pathways enriched in the differentially expressed genes after GMFB treatment (Fig. S2).

The induction of ferroptosis was verified with a series of experiments and was rescued by the ferroptosis inhibitor liproxtatin-1 (Fig. 2). Through the application of the lysosome inhibitor BafA1 and the activator NKH477, we found an essential role of autophagy in resisting ferroptosis and that GMFB decreased the acidity and activity of lysosomes, which led to ACSL4 accumulation and ferroptosis in RPE cells (Fig. 4). ACSL4 is one of the substrates of chaperone-mediated autophagy, which can be identified by HSC70 and degraded in the lysosome (Fig. 5). Similar to the hypothesis, CMA activation rescued GMFB-induced ferroptosis and early diabetic retinopathy.

Müller glia are the major glial component of the retina and respond rapidly to retinal injury in a variety of ways that can be either protective or detrimental to retinal function [41]. It has been well established that Müller cells become activated in diabetes, and most of the growth factors, cytokines, and chemokines released by Müller cells have been identified in the vitreous of diabetic patients [42,43]. Herein, we found that the GMFB concentration in the medium of Müller cells was significantly increased after high glucose treatment (Fig. 1B). During diabetes, Müller cells may secrete GMFB into the vitreous or affect retinal cells through direct cell–cell communications to regulate their metabolism and physiological activity.

The role of GMFB in the retina is rarely studied, and most research focuses on the effect of intracellular GMFB [44]. Here, in our research, extracellular GMFB may play a role as a stress protein to influence autophagy and ferroptosis of RPE cells and subsequent physiological functions. In addition, GMFB in the vitreous increased rapidly as early as one day after STZ injection, but most studies on DR focus on the late stage, and treatment methods such as anti-inflammatory drugs, laser photocoagulation, and vitrectomy are also designed for advanced microvascular disease. Our research on GMFB is a further study on the early pathogenesis of DR to serve as a new therapeutic target for the treatment of DR and other retinal diseases.

There are few studies about the role of ferroptosis in retina-related disease, and most of them focus on the effects of artificially added reagents (tBH, BSO, erastin, etc.) on cell sensitivity against ferroptosis [13–16]. However, in our research, extracellular GMFB increased during diabetes and could directly induce ferroptosis in RPE cells. Previous researchers have reported the activation of ferroptosis by autophagy, such as ferritinophagy, lipophagy, clockophagy, and GPX4-selective autophagy [10]. However, a series of papers also suggested that autophagy may play an inhibitory role in ferroptosis.

Recently, Mathieu Bourdenx et al. [45] imposed CMA loss on a mouse model of Alzheimer's disease (AD) and found that the modified proteins were mainly enriched in lipid metabolism after Gene Ontology analysis. Moreover, through genome-wide CRISPRi/a screens, Ruilin Tian et al. [46] first found that knockdown of lysosomal or autophagy-related proteins strongly sensitizes neurons to oxidative stress by generating reactive oxygen species and triggering ferroptosis. In particular, loss of saposins in PSAP-KO neurons blocks glycosphingolipid degradation in lysosomes, leading to the formation of lipofuscin, which in turn accumulates iron and generates peroxidized lipids. Here, we found that the impairment of lysosome acidification and autophagic flux caused by BafA1 or GMFB induced ferroptosis. As a direct inhibitor of GPX4 and a synthetase of lethal lipid species, ACSL4

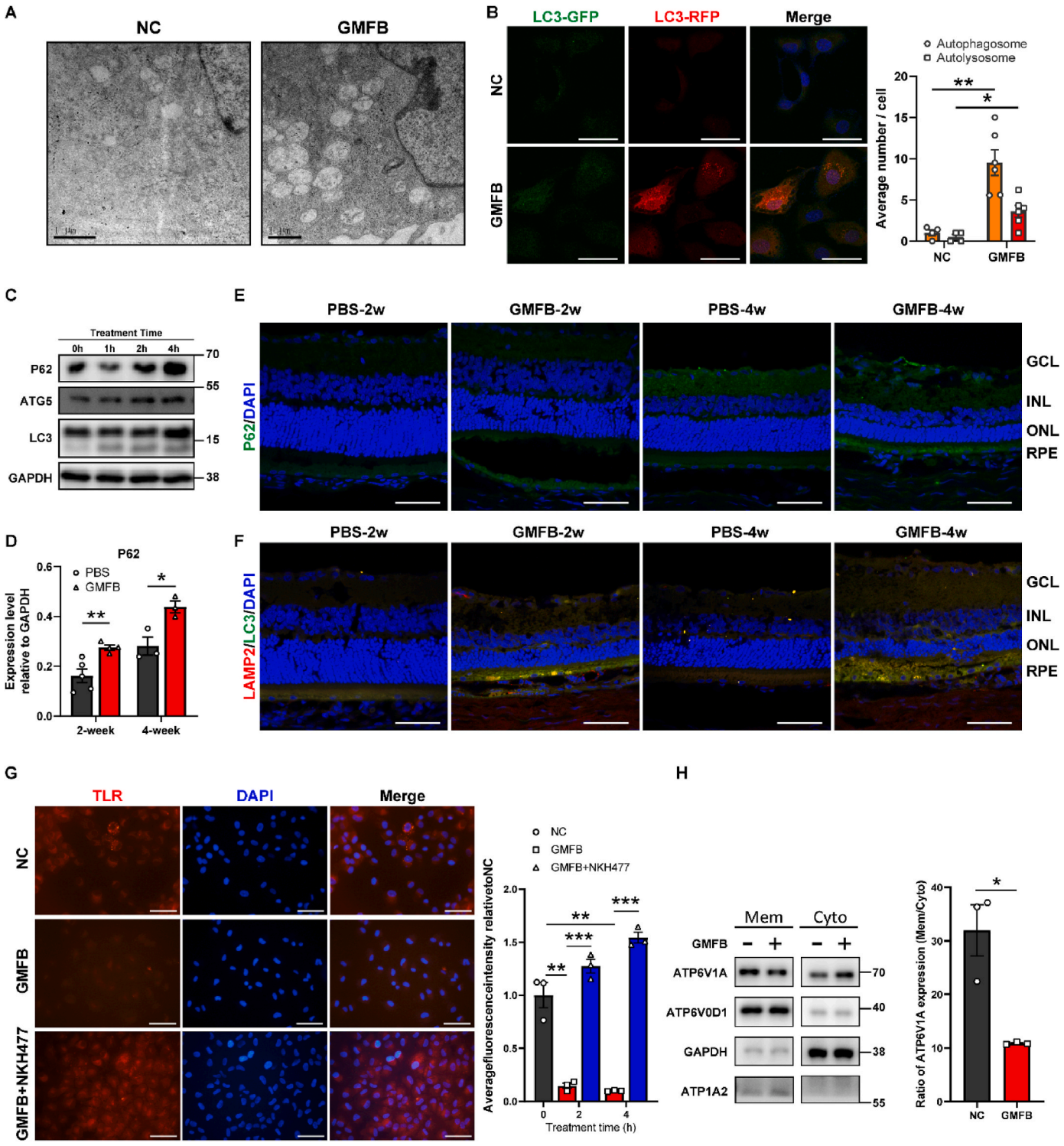

Fig. 3. Extracellular GMFB induces lysosome dysfunction and autophagy blockage in RPE cells

(A) Visualization of autophagic vacuoles in GMFB-treated ARPE19 cells by TEM. (B) The autophagy level detected with mRFP-GFP-LC3 ARPE19 cells after GMFB treatment for 4 h. Scale bar marks 20 μm. (C) The expression level of autophagy relative protein in ARPE19 cells after treatment with 0.01 μg/μL GMFB for different time. (D) The expression of P62 in the SD Rats' retina after GMFB injection detected by western-blot. (E–F) The expression pattern of autophagy relative protein in the SD Rats' retina after injection with GMFB for different time. (E)P62; (F) LC3 and LAMP2. Scale bar marks 50 μm. (G)The acidification of lysosome detected with Lysosome Tracker Red after GMFB treatment with/without NKH477. Scale bar marks 20 μm. (H) The expression of two main lysosome ATPase (ATP6V1A and ATP6V0D1) in membrane and cytoplasm after GMFB treatment for 4 h.

Data are presented as means ± SEM of at least three independent experiments. *$p < 0.05$, **$p < 0.01$ and ***$p < 0.001$ versus the control with the same treatment (Student's t-test). (For interpretation of the references to colour in this figure legend, the reader is referred to the Web version of this article.)

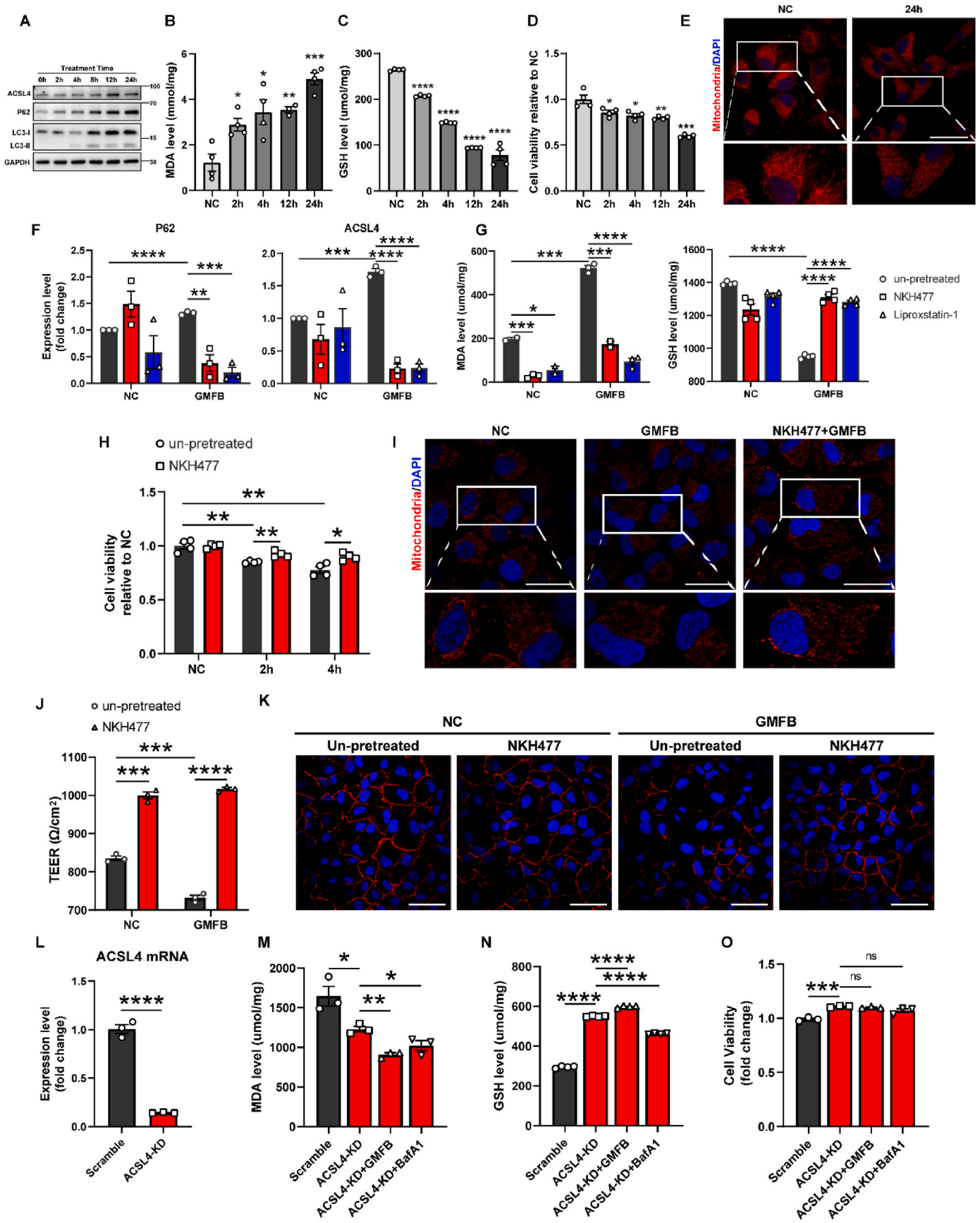

(caption on next page)

Fig. 4. GMFB-induced lysosome dysfunction leads to ferroptosis through ACSL4 accumulation
(A) The expression of autophagy relative protein and ACSL4 in BafA1-treated ARPE19 cells. (B) The cell viability of ARPE19 after BafA1 treatment detected with CCK-8. (C–D) The MDA and GSH level in ARPE19 cells after BafA1 treatment. (E) Active mitochondria stained with Chloromethyl-X-rosamine in BafA1-treated ARPE19 cells. (F) The expression of ACSL4 and P62 in ARPE19 cells after GMFB treatment with NKH477 or Liproxstatin-1 detected through western-blot. (G) The MDA and GSH level in ARPE19 cells after GMFB treatment with NKH477 or Liproxstatin-1. (H) The cell viability of ARPE19 cells after GMFB treatment with/without NKH477. (I) Active mitochondria stained with Chloromethyl-X-rosamine after GMFB treatment with/without NKH477. (J) TEER of ARPE19 cells after GMFB treatment with/without NKH477. (K) Immunofluorescence results of ZO-1 in ARPE19 cells after GMFB treatment with/without NKH477. (L) The expression of ACSL4 mRNA in ARPE19 cells after siRNA transfection for 24 h. (M − N) The MDA and GSH level in ACSL4-KD ARPE19 cells after GMFB or BafA1 treatment for 4 h. (O) The cell viability of ACSL4-Knock down (ACSL4-KD) ARPE19 cells after GMFB or BafA1 treatment for 4 h.
Data are presented as means ± SEM of at least three independent experiments. *$p < 0.05$, **$p < 0.01$, ***$p < 0.001$ and ****$p < 0.0001$, versus the control with the same treatment (Student's t-test).

can be degraded under normal conditions in RPE cells via the CMA pathway and can accumulate due to GMFB-induced lysosomal dysfunction. Further studies are required to shed more light on the complex molecular mechanisms, which could help researchers understand the relationship between ferroptosis and autophagy.

Although the functional mechanisms of extracellular GMFB have been intensively studied in the current study, there are still some limitations to be considered. For example, it has been shown that the antioxidative protein GPX4 can also be degraded via the CMA pathway [40], and we also found here that the expression of both ACSL4 and GPX4 was upregulated in the retina after GMFB injection. How cells maintain a balance between degradation substrates that play different roles remains to be studied. Moreover, the vitreous is separated from the RPE by the retina, and the vitreous content may be only a detectable indicator rather than a source that would act on the RPE. GMFB may be secreted into the vitreous and thus penetrate into the RPE layer or affect RPE cells through direct cellular interactions. We have only applied methods of vitreous injection and direct treatment to study the effects of GMFB, and potential cell–cell communication remains to be explored. Fortunately, regardless of the pathway through which GMFB exerts its effects, targeted antibody injections in the vitreous had a significant protective effect on retinal function. Furthermore, as an indicator, the level of GMFB in the vitreous is expected to be a molecular biomarker for early DR diagnosis.

4. Materials and methods

- Reagents and antibodies

Autophagy Indicator (HB-AP210-0001) was purchased from HanBio (Shanghai, China). Recombinant human GMFB Protein (Cat: 13244-HNAE) was purchased from Sino Biological. Streptozotocin (STZ, S0130) was supplied by Sigma-Aldrich (St. Louis, MO). DMEM-F12 medium (11330032) was purchased from HyClone (Logan, UT). Penicillin/Streptomycin (15140155) was purchased from Invitrogen (Carlsbad, CA). BCA Protein Quantification Kit (20201ES76) and PAGE Gel Quick Preparation Kit (12.5%) (20326ES62) was purchased from YEASEN (Shanghai, China). Liproxstatin-1 (S7699), Bafilomycin A1 (S1413), Cycloheximide (S7418), Chloroquine (S6999) and MG-132 (S2619) were purchased from Selleck. NKH477 (T16332) and QX77 (T4663) were purchased from TopScience. The primary antibody against LC3A/B (D3U4C) (#12741) was purchased from Cell Signaling Technology. 4-Hydroxynonenal Antibody (MAB3249) was purchased from R&D Systems. ZO-1 Polyclonal antibody (21773-1-AP), RPE65 Polyclonal antibody (17939-1-AP), P62/SQSTM1 Antibody (18420-1-AP), ACSL4/FACL4 Polyclonal antibody (22401-1-AP), GPX4 Polyclonal antibody (14432-1-AP), Hsc70 Polyclonal antibody (10654-1-AP), LAMP2 Monoclonal antibody (66301-1-Ig), HRP-conjugated GAPDH Monoclonal antibody (HRP-60004), HRP-conjugated Beta Actin Monoclonal antibody (HRP-60008), Cy3 conjugated Goat Anti-Mouse IgG (H + L) (SA00009-1), Cy3 conjugated Goat Anti-Rabbit IgG (H + L) (SA00009-2), FITC conjugated Goat Anti-Rabbit IgG (H + L) (SA00003-2) were purchased from Proteintech. *Trans*-well insert (0.4 μm) was purchased from Millipore (Billerica, MD). Protease Inhibitor Cocktail (K1019) was purchased from APExBIO. FerroOrange was purchased from Dojindo Molecular Technology (Japan). The protein extraction RIPA buffer (P0013B), CCK-8 solution (C0037), ROS detection solution (S0033) and Lyso-Tracker Red (C1046) were purchased from Beyotime Institute of Biotechnology (Jiangsu, China).

- Experimental animals and intravitreal injection

Male Sprague-Dawley rats weighing 120–160 g were purchased from Slaccas (Shanghai, China). The rats were treated in accordance with the ARVO Statement for the Use of Animals in Ophthalmic and Vision Research and The Guides for the Care and Use of Animals (National Research Council and Tongji University). The protocol was approved by the Committee on the Ethics of Animal Experiments of Tongji University (Permit Number: TJAA09620202). The rats were divided into 3 groups, namely, normal control (NC), GMFB-injected (GMFB), diabetes mellitus (STZ). Diabetes mellitus was induced by intraperitoneal injection of streptozotocin (STZ, 60 mg/kg; Sigma-Aldrich, St. Louis, MO, USA) after overnight fasting. For GMFB group, GMFB (0.2μg/eye, 4 μL) or equal volume of PBS was injected intravitreally. The rats were killed after different time, the vitreous and RPE-Bruch's membrane choriocapillaris complexes (RBCCs) were isolated for the subsequent assay.

- Enzyme Linked Immunosorbent Assay (ELISA)

The concentration of GMFB protein in rats' vitreous was determined through Enzyme Linked Immunosorbent Assay (ELISA) using commercially available kits from Elabscience according to the manufacturer's instructions.

- Immunofluorescence staining and TUNEL assay

Cryostat sections and ARPE-19 cells were fixed with cold 4% polyformaldehyde overnight, and permeabilized in 1x PBS containing 0.5% Triton X-100 for 10 min. For TUNEL assay, the slides were incubated in TUNEL reaction mix containing nucleotides and terminal deoxynucleotidyl transferase (TdT) at 37 °C for 1 h. For immunofluorescence staining, after blocking in PBS containing 3% BSA for 1 h, the slide and cells were then incubated with the primary antibodies overnight. A sample without primary antibody served as the negative control. After the secondary antibody incubation and DAPI staining, the slides and cells were mounted with coverslips by using Dako and examined with Nikon microscope (Nikon A1R). Exposure conditions in the same channel of different groups in each experiment were consistent.

- ERG

Retinal functions were examined with ERG, using an AVES-2000 electrophysiological apparatus (Kanghuaruiming S&T). A positive electrode was placed in the subcutaneous position between the two ears, while negative electrodes were contacted on the surface of the cornea. The two eyes were stimulated simultaneously twice at flash intensity of 0.06325 cd × s/m2, which allowed the response of the retina to be recorded.

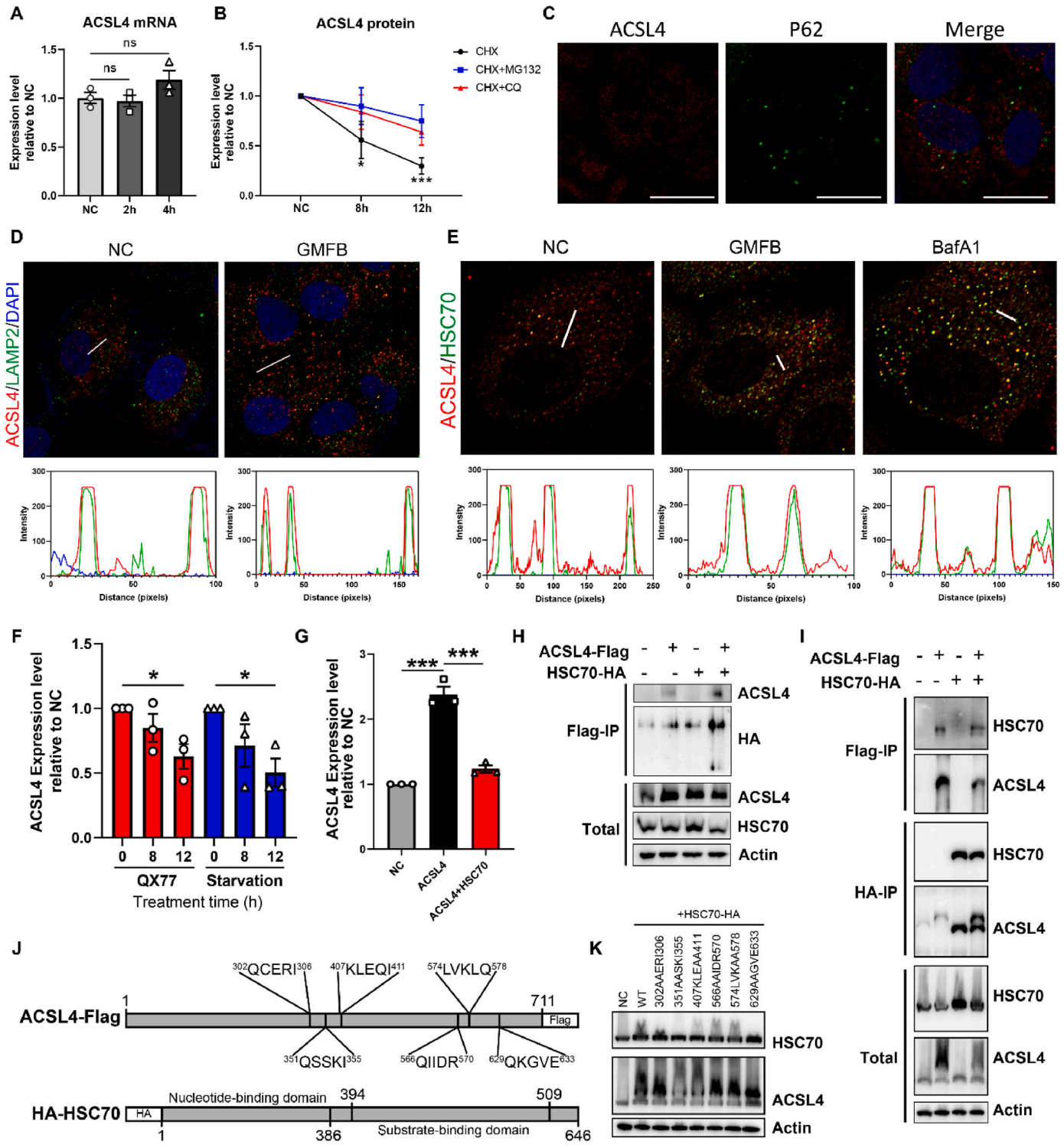

Fig. 5. ACSL4 is the substrate of chaperone-mediated autophagy

(A) The expression of ACSL4 mRNA in ARPE19 cells after GMFB treatment. (B) The expression of ACSL4 protein in ARPE19 cells after CHX treatment with CQ or MG132. (C) Immunofluorescence staining of ACSL4 and P62 in ARPE19 cells after GMFB treatment. Scale bar marked 10 μm. (D–E) Immunofluorescence co-localization analysis of ACSL4 and LAMP2A or HSC70 in ARPE19 cells after GMFB treatment. (F) The expression of ACSL4 protein in ARPE19 cells after treatment with CMA activator QX77 or culture medium without FBS. (G) The expression of ACSL4 protein in ARPE19 cells after transfection with ACSL4- and HSC70-overexpression plasmid. (H) The immunoprecipitation result of ACSL4-Flag and HSC70-HA protein in ARPE19 cells. (I) The immunoprecipitation result of ACSL4-Flag and HSC70-HA protein in 293T cells. (J) Schematic diagram of recombinant protein ACSL4-Flag and HA-HSC70 and the possible HSC70 binding sites ("KFERQ" motif) in the sequence of human ACSL4 protein. (K) The expression of wildtype/mutant ACSL4 protein in 293T cells after co-transfection with HSC70-HA plasmid. Data are presented as means ± SEM of at least three independent experiments. *p < 0.05, **p < 0.01, ***p < 0.001, versus the control with the same treatment (Student's t-test).

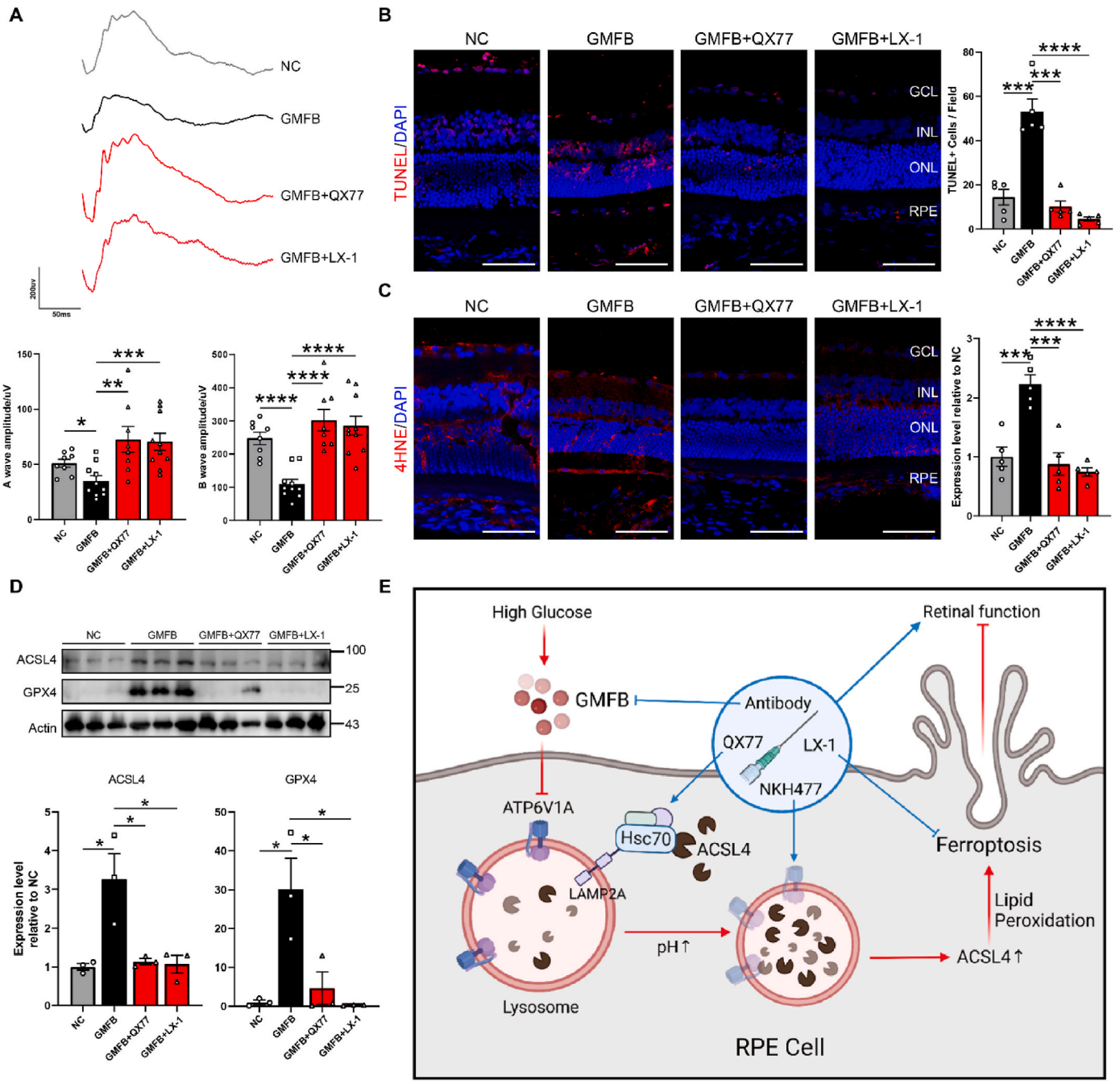

Fig. 6. Retinal dysfunction induced by GMFB can be rescued with the CMA activator QX77 or the ferroptosis inhibitor LX-1
(A) The ERG result after GMFB injection with QX77 or LX-1 in normal SD rats' vitreous for 2 weeks. (B) TUNEL-staining results of the SD Rats' retina after GMFB injection with QX77 or LX-1 for 2 weeks. Scale bar marks 50 μm. (C) Immunofluorescence results of 4-HNE in the SD Rats' retina after GMFB injection with QX77 or LX-1 for 2 weeks. Scale bar marks 50 μm. (D) The expression of ACSL4 and GPX4 in the SD Rats' RPE-Bruch's membrane-choriocapillaris complex (RBCC tissue) after GMFB injection with QX77 or LX-1 for 2 weeks. (E) The function mechanism of GMFB in the induction of RPE ferroptosis in early diabetic retinopathy. Created with BioRender.com. Data are presented as means ± SEM of at least three independent experiments. *$p < 0.05$, **$p < 0.01$, ***$p < 0.001$ and ****$p < 0.0001$, versus the control with the same treatment (Student's t-test).

- Cell culture and treatment

The ARPE19 cells were maintained respectively in Dulbecco's Modified Eagle Medium/Nutrient Mixture F-12 containing 10% fetal bovine serum, penicillin (90 units/mL) and streptomycin (0.09 mg/mL). The rat Müller and 293T cell lines were maintained in Dulbecco's Modified Eagle Medium/High Glucose containing 10% fetal bovine serum, penicillin (90 units/mL) and streptomycin (0.09 mg/mL). Cells were grown at 37 °C in a humidified atmosphere of 5% CO2 and 95% air. To establish the in vitro cell model, ARPE19 cell line were treated with 0.01μg/uL GMFB (cat. no. 13244-HNAE; Sino Biological) and untreated ARPE19 was used as the control.

- Transmission electron microscopy (TEM)

The GMFB-treated ARPE-19 cells were collected centrifugally and fixed with glutaraldehyde at 4 °C overnight. After washing with phosphate buffer, fixation was performed using osmium acid for 2 h,

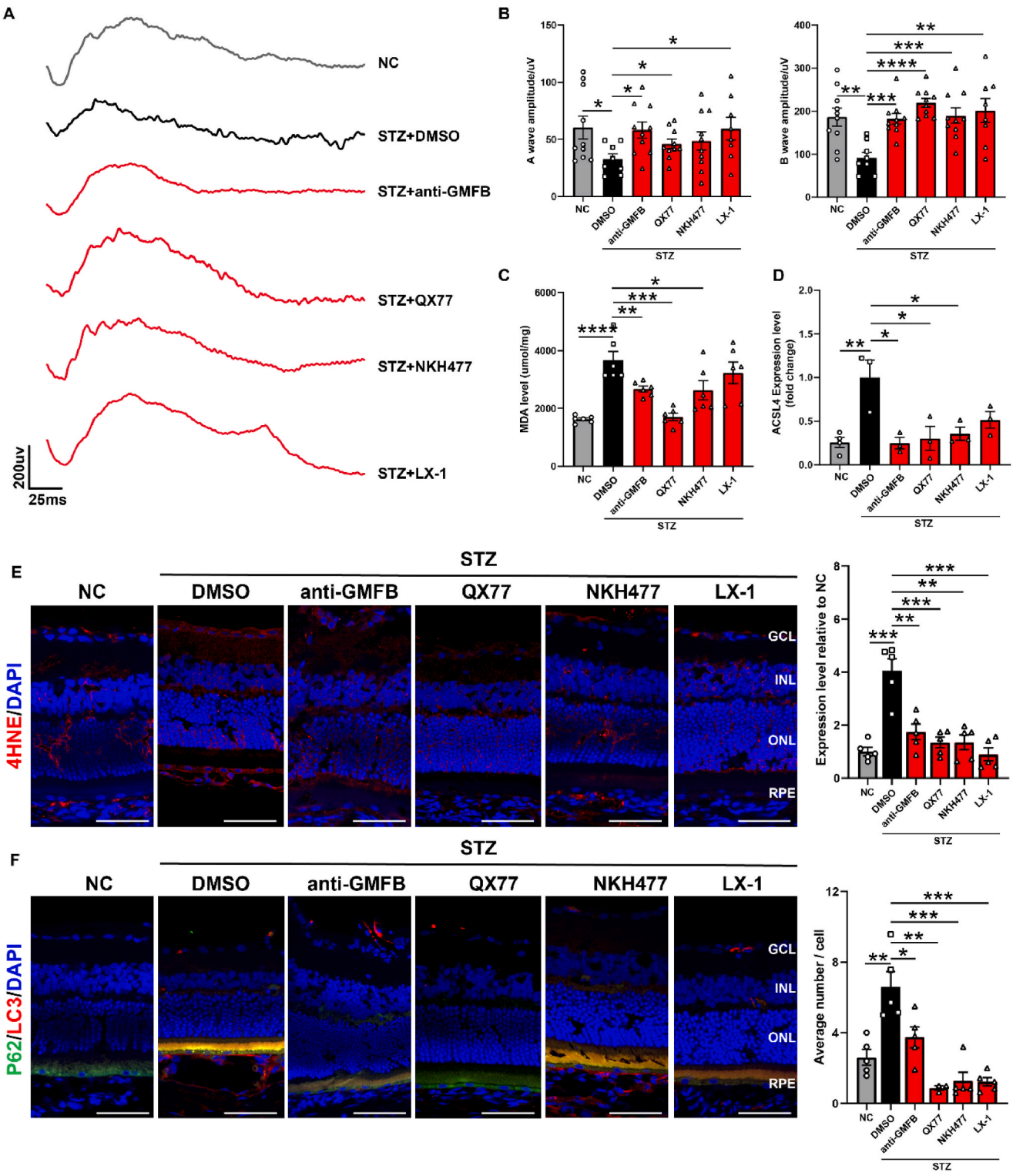

Fig. 7. GMFB antibody, QX77, NKH477, and LX-1 protects against DR

(A-B) The ERG result after injection of GMFB antibody, QX77, NKH477, LX-1 or equal volume of DMSO in diabetic rats' vitreous for 2 weeks. (C) The MDA level in the retina after injection of GMFB antibody, QX77, NKH477, LX-1 or equal volume of DMSO in diabetic rats' vitreous for 2 weeks. (D) The expression of ACSL4 in the RBCC tissue after injection of GMFB antibody, QX77, NKH477, LX-1 or equal volume of DMSO in diabetic rats' vitreous for 2 weeks. (E) The expression pattern and relative quantification of 4HNE in the retina after injection of GMFB antibody, QX77, NKH477, LX-1 or equal volume of DMSO in diabetic rats' vitreous for 2 weeks. Scale bar marks 50 μm. (F) The expression pattern of P62 and LC3 in the retina as well as the statistical figure of autophagosome (yellow spot) after injection of GMFB antibody, QX77, NKH477, LX-1 or equal volume of DMSO in diabetic rats' vitreous for 2 weeks. Scale bar marks 50 μm.

Data are presented as means ± SEM of at least three independent experiments. *$p < 0.05$, **$p < 0.01$, ***$p < 0.001$ and ****$p < 0.0001$, versus the control with the same treatment (Student's t-test). (For interpretation of the references to colour in this figure legend, the reader is referred to the Web version of this article.)

followed by dehydration using acetone gradient. The samples were embedded using EPON and sectioned after high temperature polymerization for 48 h. Ultrathin sections (50 nm thick) were cut, and stained with uranyl acetate and lead citrate. Pictures were finally examined by TEM microscopy (JEM-1230, JEOL, Japan).

- Transepithelial electrical resistance (TEER) measurement

ARPE-19 cells were plated on Millicell Hanging Cell Culture Insert (PET 0.4 μm, 24-well) and treated with 0.01 μg/μL GMFB for 4 h. Transepithelial electrical resistance (TEER) was measured with the Millicell ERS-2 (Electrical Resistance System) according to the manufacturer's instructions. The resistance is presented as absolute values (Ohm × cm^2).

- RNA-seq and GSEA analysis

After GMFB treatment, total RNA in cells was extracted and RNA-seq was performed by BGI Tech (Shenzhen, China) using the Illumina HiSeq TM 2000 platform. The gene expression was quantified with RPKM algorism (Reads Per Kb per Million reads) [47] and annotated based on the human reference genome GRCh38. To identify genomic features associated with GMFB treatment, gene set enrichment analysis (GSEA) was performed using the standard GSEA tool [48]. Analyses were performed to identify gene sets that were enriched in GMFB-treated ARPE19 cells relative to untreated cells. Gene sets were considered significantly enriched if their false discovery rate (FDR) q-value was <0.25 and nominal p-value < 0.05, as defined by the publishers of the GSEA tool.

- CCK8 cells viability assay

The ARPE19 cells were seeded into 96-well plates with concentration of 2×10^3 cells/well and incubated at 37 °C in a humidified atmosphere of 5% CO2 and 95% air. After treatment with GMFB for different time, CCK-8 solution (C0037, Beyotime) was added to each well and incubated for 2 h. The optical density (OD) values were measured with a microplate reader (Bio-Tek) at 450 nm.

- Lipid Peroxidation MDA assay

The MDA level was determined with Lipid Peroxidation MDA assay kit (S0131, Beyotime, China) following the manufacture's instruction. After GMFB treatment for 2–4 h, cell lysates were prepared and centrifuged at 10,000 g for 10 min to remove debris. The supernatant was subjected to the measurement of MDA levels and the protein contents, and the intracellular levels of MDA were calculated based on cellular protein concentration.

- Total GSH Assay

The concentration of intracellular GSH was determined with Total Glutathione Assay Kit (S0052, Beyotime, China) following the manufacture's instruction. After GMFB treatment for 2–4 h, cell lysates were prepared and reacted with assay solution for 25 min at 25 °C. The absorbance at 412 nm was measured on Spectra Max M5 microplate reader. The intracellular levels of GSH were calculated based on the weight of cell lysates.

- Mitochondrial Potential Determination

Mitochondria membrane potential was determined with Mito-Tracker Red CMXRos (C1035, Beyotime, China) following the manufacture's instruction. After GMFB treatment for 2–4 h, cells were loaded with 200 nM working solution for 20 min at 37 °C, and the fluorescence changes were then determined under confocal microscope.

- Lysosome acidity detection

The ARPE19 cells were seeded into 96-well plates with concentration of 2×10^3 cells/well and incubated at 37 °C in a humidified atmosphere of 5% CO2 and 95% air. After treatment with GMFB for different time, Lyso-Tracker Red (1:15000, cat. no. C1046; Beyotime) was added to each well and incubated for 30 min. The acidity and activity of lysosome was measured with fluorescence microscope.

- Protein extraction and Western-blot

ARPE19 whole-cell lysates were prepared for Western blotting by radioimmunoprecipitation assay lysis buffer (P0013B, Beyotime) for total protein analysis. For membrane protein analysis, cells were lysised with Membrane and Cytoplasmic Protein Extraction Kit (P0033, Beyotime). After protein concentrations determination, equal amounts (20 μg) of protein were loaded to SDS-PAGE gels and transferred electrophoretically onto a PVDF membrane (Bio-Rad, Hercules, CA, USA). After blocking with 3% BSA, the membranes were then incubated with the primary antibodies overnight. After visualization by enhanced chemiluminescence (Millipore), the optical density of each band was determined (GelPro software).

- mRFP-GFP-LC3 cell model construction

Autophagy Indicator mRFP-GFP-LC3 (HB-AP210-0001) was purchased from HanBio (Shanghai, China). Adenoviral infection was performed according to the manufacturer's instructions. ARPE19 cells grown in the concentrations of 50–70% were incubated in medium with the adenoviruses for 6 h, subsequently in complete DMEM-F12 medium containing 1000x Puromycin for 24–48 h. Based on different pH stability, the fluorescent signal of GFP could be quenched under the acidic condition inside the lysosome, while the mRFP fluorescent signal has no significant change. Autophagic flux can be observed or determined by evaluating the number of GFP and mRFP puncta in merged images.

- siRNA knockdown

For knock-down experiments, ARPE19 cells were seeded at 50%–60% confluence in six-well tissue culture plate and grown overnight. Cells were transfected with double-stranded inhibitory RNA oligonucleotides (Sangon Biotech (Shanghai) Co., Ltd.) using Lipofectamine 3000 (Invitrogen, USA) according to the manufacturer's instructions. RT-qPCR and Western blot analyses were carried out to confirm the specific inhibitory activity.

- Plasmid transfection and site-specific mutagenesis

HEK293T and ARPE19 cells were transfected with cDNAs for HSC70 (HG11329-NY, SinoBiological) and ACSL4 (P21772, MiaoLing Plasmid Platform) using jetPRIME reagent (114-01, Polyplus Transfection). Mutant versions of ACSL4 cDNA plasmid were generated using site-directed mutagenesis with Mut Express II Fast Mutagenesis Kit (C214-01, Vazyme), according to the manufacturer's instructions.

- RT-qPCR

Total RNA was extracted and reverse transcription was performed using the Primescript™ RT Master Mix kit (Takara, Shiga, Japan). Real-time PCR was performed in a Chromo4 instrument cycler (Bio-Rad, Hercules, USA) using SuperReal Premix plus (SYBR green) kit (Tiangen Biotech, Beijing, China). PCR amplification was carried out in triplicate with the following cycling parameters: denaturation at 95 °C for 5 min, followed by 40 cycles of 95 °C for 30 s, 60 °C for 40 s.

- Statistical analysis

All experiments were repeated at least three times. Data were expressed as mean ± SEM. The statistical analysis was carried out by using least significant difference test after One-way ANOVA; a P-value of 0.05 or less was considered statistically significant.

Author contributions

C.L., L.L., H.T. and G.X conceived, developed and mentored the project. C.L performed the experiments. W.S., T.Z., S.S., J.Z., H.T., J.X., C.J., F.G., J.L, J.W. and W.L provided technical support and analyzed the data. C.L, and L.L wrote the manuscript. All authors read and approved the final manuscript.

Ethics statement

All animal protocols were in accordance with the ARVO Statement for the Use of Animals in Ophthalmic and Vision Research and The Guides for the Care and Use of Animals (National Research Council and Tongji University) (Permit Number: TJmed-010-32).

Declaration of competing interest

The authors declare that they do not have any commercial or associative interest that represents a conflict of interest in connection with the work submitted.

Acknowledgments

This work was supported by grants from the National Natural Science Foundation of China (31201108), the Ministry of Science and Technology of China (2020YFA0113101) and the Fundamental Research Funds for the Central Universities (22120220009).

Appendix A. Supplementary data

Supplementary data to this article can be found online at https://doi.org/10.1016/j.redox.2022.102292.

References

[1] A.W. Stitt, T.M. Curtis, M. Chen, et al., The progress in understanding and treatment of diabetic retinopathy, Prog. Retin. Eye Res. 51 (2016 Mar) 156–186.
[2] F. Bandello, R. Lattanzio, I. Zucchiatti, et al., Pathophysiology and treatment of diabetic retinopathy, Acta Diabetol. 50 (1) (2013) 1–20.
[3] D. Tonade, T.S. Kern, Photoreceptor cells and RPE contribute to the development of diabetic retinopathy, Prog. Retin. Eye Res. 83 (2021 Jul), 100919.
[4] O. Strauss, The retinal pigment epithelium in visual function, Physiol. Rev. 85 (3) (2005) 845–881.
[5] K. Kaarniranta, P. Tokarz, A. Koskela, et al., Autophagy regulates death of retinal pigment epithelium cells in age-related macular degeneration, Cell Biol. Toxicol. 33 (2) (2017) 113–128.
[6] W. Lin, G. Xu, Autophagy: a role in the apoptosis, survival, inflammation, and development of the retina, Ophthalmic Res. 61 (2) (2019) 65–72.
[7] B. Villarejo-Zori, J.I. Jimenez-Loygorri, J. Zapata-Munoz, et al., New insights into the role of autophagy in retinal and eye diseases, Mol. Aspect. Med. 82 (2021 Dec), 101038.
[8] S. Kume, Autophagy as a therapeutic target in diabetic nephropathy 2012 (12) (2012), 628978.
[9] W. Wang, Q. Wang, D. Wan, et al., Histone HIST1H1C/H1.2 regulates autophagy in the development of diabetic retinopathy, Autophagy 13 (5) (2017 May 4) 941–954.
[10] X. Chen, J. Li, R. Kang, et al., Ferroptosis: machinery and regulation, Autophagy (2020 Aug 26) 1–28.
[11] J.J. Peng, W.T. Song, F. Yao, et al., Involvement of regulated necrosis in blinding diseases: focus on necroptosis and ferroptosis, Exp. Eye Res. 191 (2020 Feb), 107922.
[12] J.J. Lee, K. Ishihara, S. Notomi, et al., Lysosome-associated membrane protein-2 deficiency increases the risk of reactive oxygen species-induced ferroptosis in retinal pigment epithelial cells, Biochem. Biophys. Res. Commun. 521 (2) (2020 Jan 8) 414–419.
[13] Y. Sun, Y. Zheng, C. Wang, et al., Glutathione depletion induces ferroptosis, autophagy, and premature cell senescence in retinal pigment epithelial cells, Cell Death Dis. 9 (7) (2018 Jul 9) 753.
[14] S. Jiang, S.E. Moriarty, H. Grossniklaus, et al., Increased oxidant-induced apoptosis in cultured nondividing human retinal pigment epithelial cells, Invest. Ophthalmol. Vis. Sci. 43 (8) (2002 Aug) 2546–2553.
[15] B.F. Godley, G.F. Jin, Y.S. Guo, et al., Bcl-2 overexpression increases survival in human retinal pigment epithelial cells exposed to H(2)O(2), Exp. Eye Res. 74 (6) (2002 Jun) 663–669.
[16] W. Shu, B.H. Baumann, Y. Song, et al., Ferrous but not ferric iron sulfate kills photoreceptors and induces photoreceptor-dependent RPE autofluorescence, Redox Biol. 34 (2020 Jul), 101469.
[17] Z. Tang, Y. Ju, X. Dai, et al., HO-1-mediated ferroptosis as a target for protection against retinal pigment epithelium degeneration, Redox Biol. 43 (2021 Jul), 101971.
[18] T. Zhou, K.K. Zhou, K. Lee, et al., The role of lipid peroxidation products and oxidative stress in activation of the canonical wingless-type MMTV integration site (WNT) pathway in a rat model of diabetic retinopathy, Diabetologia 54 (2) (2011 Feb) 459–468.
[19] A. Sharma, R. Sharma, P. Chaudhary, et al., 4-Hydroxynonenal induces p53-mediated apoptosis in retinal pigment epithelial cells, Arch. Biochem. Biophys. 480 (2) (2008 Dec 15) 85–94.
[20] Y. Liu, D. Zhang, Y. Wu, et al., Docosahexaenoic acid aggravates photooxidative damage in retinal pigment epithelial cells via lipid peroxidation, J. Photochem. Photobiol., B 140 (2014 Nov) 85–93.
[21] C. Liu, T. Zhu, J. Zhang, et al., Identification of novel key molecular signatures in the pathogenesis of experimental diabetic retinopathy, IUBMB Life 73 (11) (2021 Nov) 1307–1324.
[22] R. Lim, A. Zaheer, M.A. Yorek, et al., Activation of nuclear factor-kappaB in C6 rat glioma cells after transfection with glia maturation factor, J. Neurochem. 74 (2) (2000 Feb) 596–602.
[23] A. Zaheer, S. Zaheer, S.K. Sahu, et al., A novel role of glia maturation factor: induction of granulocyte-macrophage colony-stimulating factor and pro-inflammatory cytokines, J. Neurochem. 101 (2) (2007 Apr) 364–376.
[24] A. Zaheer, S. Knight, A. Zaheer, et al., Glia maturation factor overexpression in neuroblastoma cells activates glycogen synthase kinase-3beta and caspase-3, Brain Res. 1190 (2008 Jan 23) 206–214.
[25] D. Kempuraj, M.M. Khan, R. Thangavel, et al., Glia maturation factor induces interleukin-33 release from astrocytes: implications for neurodegenerative diseases, J. Neuroimmune Pharmacol. 8 (3) (2013 Jun) 643–650.
[26] J. Fan, T. Fong, X. Chen, et al., Glia maturation factor-β: a potential therapeutic target in neurodegeneration and neuroinflammation, Neuropsychiatric Dis. Treat. 14 (2018) 495–504.
[27] M. Nieto-Sampedro, R. Lim, D.J. Hicklin, et al., Early release of glia maturation factor and acidic fibroblast growth factor after rat brain injury, Neurosci. Lett. 86 (3) (1988 Apr 12) 361–365.
[28] R. Lim, J.F. Miller, A. Zaheer, Purification and characterization of glia maturation factor beta: a growth regulator for neurons and glia, Proc. Natl. Acad. Sci. U. S. A. 86 (10) (1989 May) 3901–3905.
[29] D.E. Turriff, R. Lim, Glia maturation factor increases cyclic GMP in glioblasts, Brain Res. 166 (2) (1979 Apr 27) 436–440.
[30] K. Totsuka, T. Ueta, T. Uchida, et al., Oxidative stress induces ferroptotic cell death in retinal pigment epithelial cells, Exp. Eye Res. 181 (2019 Apr) 316–324.
[31] A. Nishiwaki, K. Asai, T. Tada, et al., Expression of glia maturation factor during retinal development in the rat, Brain. Res. Mol. Brain. Res. 95 (1–2) (2001 Nov 1) 103–109.
[32] S.J. Dixon, K.M. Lemberg, M.R. Lamprecht, et al., Ferroptosis: an iron-dependent form of nonapoptotic cell death, Cell 149 (5) (2012 May 25) 1060–1072.
[33] D.J. Colacurcio, R.A. Nixon, Disorders of lysosomal acidification-The emerging role of v-ATPase in aging and neurodegenerative disease, Ageing Res. Rev. 32 (2016 Dec) 75–88.
[34] C.F. Kan, A.B. Singh, D.M. Stafforini, et al., Arachidonic acid downregulates acyl-CoA synthetase 4 expression by promoting its ubiquitination and proteasomal degradation, J. Lipid Res. 55 (8) (2014 Aug) 1657–1667.
[35] Z. Bao, Y. Liu, B. Chen, et al., Prokineticin-2 prevents neuronal cell deaths in a model of traumatic brain injury, Nat. Commun. 12 (1) (2021 Jul 9) 4220.
[36] L. Galluzzi, E.H. Baehrecke, A. Ballabio, et al., Molecular definitions of autophagy and related processes, EMBO J. 36 (13) (2017 Jul 3) 1811–1836.
[37] S. Kaushik, A.M. Cuervo, The coming of age of chaperone-mediated autophagy, Nat. Rev. Mol. Cell Biol. 19 (6) (2018 Jun) 365–381.
[38] J.F. Dice, Chaperone-mediated autophagy, Autophagy 3 (4) (2007 Jul-Aug) 295–299.
[39] F. Ursini, M. Maiorino, M. Valente, et al., Purification from pig liver of a protein which protects liposomes and biomembranes from peroxidative degradation and exhibits glutathione peroxidase activity on phosphatidylcholine hydroperoxides, Biochim. Biophys. Acta 710 (2) (1982 Feb 15) 197–211.
[40] Z. Wu, Y. Geng, X. Lu, et al., Chaperone-mediated autophagy is involved in the execution of ferroptosis, Proc. Natl. Acad. Sci. U. S. A. 116 (8) (2019 Feb 19) 2996–3005.
[41] D. Goldman, Muller glial cell reprogramming and retina regeneration, Nat. Rev. Neurosci. 15 (7) (2014 Jul) 431–442.
[42] D.G. Puro, Diabetes-induced dysfunction of retinal Muller cells, Trans. Am. Ophthalmol. Soc. 100 (2002) 339–352.
[43] B.A. Coughlin, D.J. Feenstra, S. Mohr, Muller cells and diabetic retinopathy, Vis. Res. 139 (2017 Oct) 93–100.
[44] J. Fan, T. Fong, X. Chen, et al., Glia maturation factor-beta: a potential therapeutic target in neurodegeneration and neuroinflammation, Neuropsychiatric Dis. Treat. 14 (2018) 495–504.

[45] M. Bourdenx, A. Martin-Segura, A. Scrivo, et al., Chaperone-mediated autophagy prevents collapse of the neuronal metastable proteome, Cell 184 (10) (2021 May 13) 2696–2714 e25.
[46] R. Tian, A. Abarientos, J. Hong, et al., Genome-wide CRISPRi/a screens in human neurons link lysosomal failure to ferroptosis, Nat. Neurosci. 24 (7) (2021 Jul) 1020–1034.
[47] A. Mortazavi, B.A. Williams, K. McCue, et al., Mapping and quantifying mammalian transcriptomes by RNA-Seq, Nat. Methods 5 (7) (2008 Jul) 621–628.
[48] A. Subramanian, P. Tamayo, V.K. Mootha, et al., Gene set enrichment analysis: a knowledge-based approach for interpreting genome-wide expression profiles, Proc. Natl. Acad. Sci. U. S. A. 102 (43) (2005 Oct 25) 15545–15550.